Journal of King Saud University – Engineering Sciences (2016) **28**, 157–164

King Saud University

Journal of King Saud University – Engineering Sciences

www.ksu.edu.sa
www.sciencedirect.com

ORIGINAL ARTICLE

Spatial moment analysis of solute transport with Langmuir sorption in a fracture–skin–matrix coupled system

N. Natarajan [a,*], **G. Suresh Kumar** [b]

[a] *Department of Civil Engineering, Indian Institute of Technology-Madras, Chennai 600036, India*
[b] *Department of Ocean Engineering, Indian Institute of Technology-Madras, Chennai 600036, India*

Received 18 October 2013; accepted 10 April 2014
Available online 19 April 2014

KEYWORDS

Fracture;
Langmuir non-linear sorption;
Fracture–skin;
Spatial moments;
Effective solute velocity and dispersion

Abstract Sorption is one of the key processes that plays a major role in the transport of contaminants in fractured porous media. Extensive studies have been conducted on sorption isotherms in fracture matrix coupled system but studies pertaining to sorption in fractured porous media with fracture–skin are very limited. In this study, a numerical model is developed for analysing the influence of sorption intensities on velocity, macro dispersion coefficient and dispersivity using the method of spatial moments. Implicit finite difference numerical technique has been used to solve the coupled non-linear governing equations. A varying grid is adopted at the fracture and skin interface to capture the mass transfer at the interface. Results suggest that the role of non-linear sorption is dominant in comparison with that of advection and dispersion in deciding the final relative concentration within the fracture. The role of sorption partition coefficients is not always enhancing the mixing phenomena which lead to dilution of solutes. Furthermore, the role of sorption partition coefficients is extremely sensitive in the sense that the resultant magnitude of effective dispersivity may either get enhanced or mitigated depending on the magnitude of sorption partition coefficients.

1. Introduction

Contaminant transport in fractured porous media has been a topic of increasing interest in recent decades as the high permeability fracture provides a preferential pathway for the movement of fluids in the subsurface medium. The quantum of diffusive mass transport along the fracture walls decides the mobility and spreading of contaminants transported along the fracture (Renu and Suresh Kumar, 2012). It is well known that the transport of reactive solutes through porous media is affected by various rate limited processes, which mainly

* Corresponding author.
E-mail addresses: itsrajan2002@yahoo.co.in (N. Natarajan), gskumar@iitm.ac.in (G. Suresh Kumar).
Peer review under responsibility of King Saud University.

Production and hosting by Elsevier

http://dx.doi.org/10.1016/j.jksues.2014.04.003

include sorption, mass transfer between regions of different velocities and transformation (Srivastava et al., 2002). Many studies have been conducted on non-linear sorption of contaminants in the porous system (Weber et al., 1991; Brusseau, 1995; Srivastava and Brusseau, 1996; Abulaban et al., 1998; Abulaban and Nieber, 2000). Sekhar et al. (2006) numerically showed that in a single fracture with matrix diffusion, the ratio between dispersivities for linearly and non-linearly sorbing solutes varies exponentially at a very large time. Suresh Kumar (2008) performed spatial moment analysis to investigate the influence of non-linear sorption intensities on dispersivity and macro-dispersion coefficients, arising from marked heterogeneities between fracture and matrix transport parameters. Earlier studies on solute transport in a fractured formation generally did not consider the presence of fracture skins. Moench (1984, 1985) defined fracture skins to be a low permeability material deposited on the fracture walls which mitigates the diffusive mass transfer between high and low permeability materials. Sharp (1993) indicated the formation of skins in fractured porous media. Later studies concluded that the fracture skins can occur as clay filling (Driese et al., 2001), mineral precipitation (Fu et al., 1994) and organic material growth (Robinson and Sharp, 1997). Thus, the formation of fracture–skin can affect the contaminant transport mechanism in fractured porous media as the properties of the fracture–skin like porosity, diffusion coefficient and retardation factor can be significantly different from that of the surrounding rock-matrix. The variation in the properties of the fracture–skin from that of the associated rock-matrix causes the diffusive mechanisms at the fracture–skin interface to be different from that of the skin–matrix interface. The thickness of the fracture–skin is generally smaller when compared to that of the rock-matrix and therefore the sorption sites available in the fracture–skin can be significantly different compared to that of the rock-matrix. Renu and Suresh Kumar (2012) have performed moment analysis on solute transport in a fracture–skin–matrix system with Freundlich sorption. Although earlier studies have only dealt with Freundlich sorption, the adsorption of a variety of chemicals from the aqueous phase of the fracture onto the rock matrix can be described by the Langmuir equilibrium sorption, including surfactants and polymers (Satter et al., 1980). Further, in a coupled fracture–matrix system, the combined influence of matrix diffusion and non-linear sorption complicates the mixing behaviour along the fracture (Suresh Kumar, 2008). In Langmuir sorption isotherm, the number of sorption sites is considered to be limited compared to Freundlich sorption isotherm. The Langmuir sorption would presumably provide a better understanding of the sorption of contaminants in the fracture–skin–matrix system as the number of sorption sites in the fracture–skin can be limited due to its limited thickness compared to the rock-matrix. The aim of this study is to analyse the influence of Langmuir sorption intensities on effective solute velocity, dispersion and dispersivity in the fracture matrix coupled system in the presence of fracture–skin using the method of moments. The mobility and spreading of solutes cannot be obtained in a straight forward manner from the spatial and temporal distribution of concentration obtained from the fracture (Renu and Suresh Kumar, 2012) and thus requires a special tool. Field, experimental and analytical solutions have their limitations in carrying out this type of study. Field studies would be time consuming and quite costly, and thus not affordable. Moreover it would take many years before we can obtain tangible results. Experiments would last for many years if the long range transport processes need to be investigated and moreover it is difficult to obtain the non-linear behaviour in a coupled fracture matrix system under various conditions involving a range of fracture and solute transport parameters (Suresh Kumar, 2008). Analytical solutions for non-linear differential equations are difficult to solve. Thus, numerical modelling along with spatial moment analysis plays an important role in deducing the concentration distribution, and further aids in quantifying the mobility and spreading of solutes along the fracture.

2. Physical system and governing equations

The conceptual model illustrating a coupled fracture–skin–matrix system (Robinson et al., 1998) is illustrated in Fig. 1. A set of parallel fractures having fracture aperture of 2b is separated by a distance of 2H. In between fracture and rock-matrix fracture–skin having thickness d–b has been considered. The principal transport mechanisms considered within the fracture include advection, hydrodynamic dispersion, sorption, and mass transfer to the adjacent skin by diffusion. Molecular diffusion, sorption and radioactive decay have been considered within the fracture–skin and rock-matrix.

The governing equation for contaminant transport in a fracture in given below (Robinson et al., 1998)

$$\frac{\partial C_f}{\partial t}+\frac{1}{b}\frac{\partial S}{\partial t}+v\frac{\partial C_f}{\partial x}-D\frac{\partial^2 C_f}{\partial x^2}-\frac{\theta_s D_s}{b}\frac{\partial C_s}{\partial y}\bigg|_{y=b}=0 \tag{1}$$

The most commonly used expression for Langmuir sorption Isotherm is given below (Singh and Srivastava, 2001; Patnaik and Das, 1995):

$$S=\frac{S_{maxf}K_aC_f}{1+K_aC_f} \tag{2}$$

where C_f is the concentration in the fracture, S_{maxf} is the maximum sorption capacity of the contaminants on the fracture wall surface, K_a is the sorption partition coefficient.

$$\frac{1}{b}\cdot\frac{\partial S}{\partial t}=\frac{1}{b}\cdot\frac{\partial S}{\partial C_f}\cdot\frac{\partial C_f}{\partial t}=\frac{1}{b}\cdot\left[\frac{S_{maxf}K_a}{1+K_aC}-\frac{S_{maxf}K_a^2C}{(1+K_aC)^2}\right]\cdot\frac{\partial C_f}{\partial t} \tag{3}$$

Substituting Eq. (3) into Eq. (1)

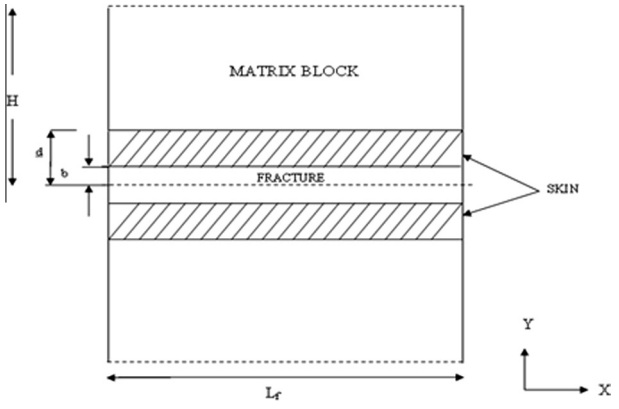

Figure 1 Schematic representation of the coupled fracture–skin–matrix system.

$$\left(1+\frac{1}{b}\left[\frac{S_{maxf}K_a}{1+K_aC}-\frac{S_{maxf}K_a^2C}{(1+K_aC)^2}\right]\right)\frac{\partial C_f}{\partial t}+v\frac{\partial C_f}{\partial x}-D\frac{\partial^2 C_f}{\partial x^2}-\frac{\theta_s D_s}{b}\frac{\partial C_s}{\partial y}\bigg|_{y=b}=0 \tag{4}$$

$$\text{where } R_f=1+\frac{1}{b}\left[\frac{S_{maxf}K_a}{1+K_aC}-\frac{S_{maxf}K_a^2C}{(1+K_aC)^2}\right] \tag{5}$$

Similarly the retardation factor for fracture skin and rock-matrix can be obtained as

$$R_s=1+\frac{\rho_s}{\theta_s}\left[\frac{S_{maxs}K_s}{1+K_sC}-\frac{S_{maxs}K_s^2C}{(1+K_sC)^2}\right] \tag{6}$$

$$R_m=1+\frac{\rho_m}{\theta_m}\left[\frac{S_{maxm}K_d}{1+K_dC}-\frac{S_{maxm}K_d^2C}{(1+K_dC)^2}\right] \tag{7}$$

where ρ_s and ρ_m are density of the fracture skin and rock matrix, S_{maxs} and S_{maxm} are the maximum sorption capacity of the contaminants within the fracture skin and rock matrix, K_s and K_d are the sorption partition coefficient within the fracture skin and rock-matrix, θ_s and θ_m are the fracture–skin and rock-matrix porosities.

In Eq. (4), R_f is the retardation factor which takes into account the Langmuir non-linear sorption within the fracture. C_f is the concentration of contaminants in the fracture, v is the average velocity of the fluid within the fracture. D is the hydrodynamic dispersion coefficient, $D=\alpha v+D^*$, α is the longitudinal dispersivity, D^* is the free molecular diffusion coefficient, b is the half fracture aperture.

The governing equation for contaminant transport in the fracture skin and rock-matrix is given as:

$$R_s\frac{\partial C_s}{\partial t}=D_s\frac{\partial^2 C_s}{\partial y^2} \tag{8}$$

$$R_m\frac{\partial C_m}{\partial t}=D_m\frac{\partial^2 C_m}{\partial y^2} \tag{9}$$

where, R_s and R_m are the retardation factors which take into account the Langmuir non-linear sorption within the fracture skin and the rock matrix, C_s and C_m are the contaminant concentration within the fracture skin and rock matrix, D_s and D_m are the fracture–skin and rock matrix diffusion coefficient.

The initial and boundary conditions associated with Eqs. (4) and (7) are:

$$C_F(x=0,t)=C_o \tag{10}$$

$$C_f(x=L_f,t)=0 \tag{11}$$

$$C_f(x,t=0)=C_s(x,y,t=0)=C_m(x,y,t=0)=0 \tag{12}$$

$$C_s(x,y=b,t)=C_f(x,t) \tag{13}$$

$$C_s(x,y=d,t)=C_m(x,y=d,t) \tag{14}$$

$$\frac{\partial C_{m(x,y=H,t)}}{\partial y}=0 \tag{15}$$

$$\frac{\theta_s D_s\partial C_s(x,y=d,t)}{\partial y}=\frac{\theta_m D_m\partial C_m(x,y=d,t)}{\partial y} \tag{16}$$

The following assumptions have been used for modelling coupled fracture–skin–matrix system.

1. The fracture aperture is much smaller than the length of the fracture.
2. Permeability of fracture–skin and rock-matrix can be ignored as there is no advection within fracture–skin and rock-matrix.
3. Concentrations at the fracture–skin interface, i.e., concentrations along the fracture walls and along the lower boundary of the fracture–skin are assumed to be equal.
4. Concentrations at the skin–matrix interface, i.e., concentration along the upper boundary of the fracture–skin and lower boundary of the rock-matrix is assumed to be equal as expressed in Eq. (14). The diffusive flux in the fracture–skin is equal to the diffusive flux in the rock-matrix at the skin–matrix interface as expressed in Eq. (16).
5. Reversible sorption within the fracture, fracture–skin and rock-matrix is accounted for by a retardation factor.
6. Due to symmetry, only one half of a high permeability fracture, its adjacent low permeability fracture–skin and its associated one half of rock-matrix has been considered for simulation.
7. Fracture skin thickness is assumed to remain constant with time.

3. Numerical method and moment analysis

In this study, the system is described by a set of partial differential equations for contaminant transport; one for the fracture, one for the fracture–skin and another for the rock-matrix, formulated for a one-dimensional framework. This coupled system of equations is solved numerically using the Upwind scheme for advection and second-order central difference finite difference scheme for dispersion. To satisfy the continuity of fluxes at the high and low permeability interface, i.e., fracture–skin interface, solution is iterated at each time step. The grid size in the fracture is maintained uniform whereas a varying grid size is adopted at the fracture–skin interface to accurately simulate the concentration flux at the fracture–skin interface. The last term on the left hand side of Eq. (4) is discretized as

$$\frac{\partial C_s}{\partial y}=\frac{C_s^{n+1}2-C_s^{n+1}1}{\Delta y(1)} \tag{17}$$

where $\Delta y(1)$ represents the cell width across the fracture–skin interface. Here the contaminant concentration in the first node in the fracture–skin, i.e., $C_s^{n+1}1$ will be equal to the corresponding fracture concentration $C_f^{n+1}1|_{i=1}$ perpendicular to the fracture–skin satisfying the boundary condition.

The contaminant concentration at the second node of the fracture–skin $C_s^{n+1}2$ is the fourth unknown in the (n + 1)th time level in Eq. (4). The value of this unknown is assumed and iterated until convergence. Thus using tridiagonal matrix algorithm (TDMA), the three unknowns are solved for the fracture at ith node, $(i+1)$th node and $(i-1)$th node at $(n+1)$th time level. Thus, the fourth unknown, the contaminant concentration at the second node of the fracture–skin

$C_s^{n+1}2$ at $(n + 1)$th time level is not solved by the TDMA as its value is assumed at $(n + 1)$th time level and iterated until convergence.

Having obtained the concentration distribution of contaminants along the fracture for a coupled fracture–skin–matrix system, at each time level, from the above numerical method, the method of spatial moments as a function of travelling time is calculated. Such spatial moments of point concentration data provide an integrated measure of the concentration field over the entire extent of the domain. In the present model, the contaminant transport parameters are considered by characterizing the three spatial moments of the concentration distribution along the fracture.

The lower order spatial moments have been obtained using a similar approach to Guven et al. (1984). The zeroth moment (M_0) is proportional to the total mass of the fluid in the high permeability fracture. The first spatial moment (M_1) describes the displacement of the centre of the mass and the second spatial moment (M_2) describes the spread of the deviation from the centre of mass. The expressions for the evaluation of the zeroth moment, first moment and second moment are given below.

$$M_n = \int_0^L x^n c(x,t)dx \tag{18}$$

$$X_1(t) = \frac{M_1}{M_0} \tag{19}$$

$$X_{11}(t) = \frac{M_2}{M_0} - \left[\frac{M_1}{M_0}\right]^2 \tag{20}$$

From these moments, the mobility and spreading of the concentration profiles can be obtained using the following expressions:

$$V(t) = \frac{d\{X_1(t)\}}{dt}, D(t) = \frac{1}{2}\frac{d\{X_{11}(t)\}}{dt} \tag{21}$$

Table 1 Parameters used in the simulation of the present study.

Parameters used for simulation	Value
Matrix diffusion coefficient (D_m)	4e-06 m^2/d
Dispersivity (α_L)	1 m
Half fracture aperture (b)	200 μm
Length of the fracture (L_f)	50 m
Total simulation time	25 days
Velocity of fluid (v)	1 m/d
Sorption partition coefficient on the fracture (K_a)	1e-04 m
Sorption partition coefficient on the rock matrix (K_d)	10 m^3/kg
Maximum sorption capacity in fracture (S_{maxf})	0.00001
Maximum sorption capacity in the rock matrix (S_{maxm})	0.01
Bulk density of matrix (ρ_s)	2000 kg/m^3
Skin diffusion coefficient (D_s)	4e-06 m^2/d
Skin porosity (θ_s)	0.035
Free molecular diffusion coefficient (D_0)	1e-06
Matrix porosity (θ_m)	0.145
Bulk density of rock-matrix (ρ_m)	2000 kg/m^3
Fracture skin thickness (d–b)	0.002 m
Maximum sorption capacity in fracture–skin (S_{maxs})	0.00001
Sorption partition coefficient on the rock matrix (K_s)	10 m^3/kg

However, the above expressions are valid for pulse sources (Maloszewski and Zuber, 1985) only. Since the boundary condition in the inlet is assumed to be a constant continuous source, a first derivative of the concentration in the fracture is used to obtain the equivalent pulse in order to use the above expressions (18)–(21).

Eq. (21) describes the expression for time dependent dispersivity as a function of time dependent macro-dispersion coefficient and time dependent velocity. Eq. (21) clearly states that the mean fluid velocity and dispersivity will not be a constant as it is applied in a typical porous medium, while it will be varying as a function of time in a coupled fracture–matrix system. It is also to be noted that Eq. (21) holds good at larger times when the coupled fracture–matrix system reaches the equilibrium condition with reference to the system heterogeneity (Suresh Kumar and Sekhar, 2005; Sekhar and Kumar, 2006; Suresh Kumar et al., 2008), while the deviations at pre-asymptotic regime reflects the significant heterogeneity associated with the coupled fracture–matrix system. Thus, during the early stages a linear relation between the macro-dispersion coefficient and the mean fluid velocity cannot be expected in a coupled fracture–matrix system as it is applied in a classical porous medium, and this departure from the linear relation is the essence of transport through fractured aquifers to be significantly different from that of a typical porous medium.

4. Results and discussion

Spatial moment analysis on solute transport with Langmuir sorption in a coupled fracture skin matrix system has been carried out in this study. The input parameters for the present study have been adopted from Robinson et al. (1998). Table 1 shows the parameters that were used for the simulation of the present study.

Fig. 2 represents the comparison of the results obtained from the present numerical model with the analytical solution provided by Robinson et al. (1998). It is observed from Fig. 2 that the present model is in close agreement with the analytical solution for contaminant transport in a fracture–matrix coupled system with fracture skin.

Fig. 3 provides spatial distribution of relative concentration along the fracture resulting from the introduction of non-linear Langmuir sorption isotherm within fracture, fracture–skin and rock-matrix for various sorption partition coefficients varying by four orders of magnitude. It can be clearly observed from Fig. 3 that the sensitivity of sorption partition coefficients is extremely critical in deciding the amount of concentration that would finally be retained within the fracture. For example, the relative concentration at a distance of 2.5 m from the inlet nearly approaches zero with $K_s = 2$; while the relative concentration is approximately 70% with $K_s = 0.0002$. Thus the role of non-linear sorption is dominant in comparison with that of advection and dispersion in deciding the final relative concentration within the fracture. In addition, it is also observed that the concentration reaches zero within 15 m from the inlet implying a very strong sorption onto the solid phase from the mobile aqueous phase.

Fig. 4 provides the temporal distribution of effective solute velocity within the high permeable fracture for various sorption partition coefficients. The effective solute velocity for the ranges of sorption partition coefficients considered in

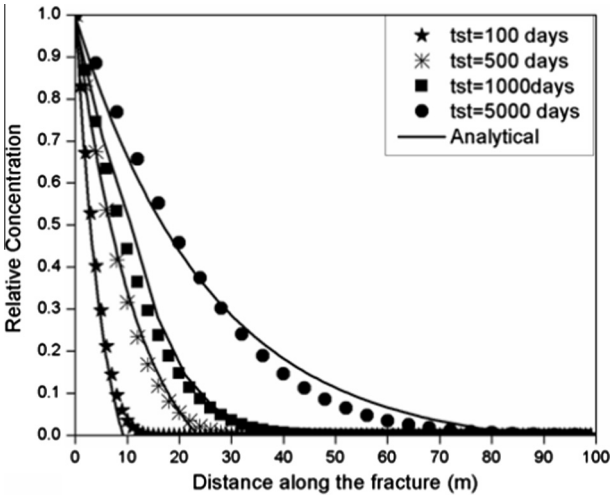

Figure 2 Comparison of numerical solution with the analytical solution for various simulation time periods for a coupled fracture–skin–matrix system.

Fig. 4 varies non-linearly implying the sensitivity of effective solute velocity with time. It is observed from Fig. 4 that the magnitude of effective solute velocities is significantly lower with reference to its mean fluid velocity of 1 m/day. In addition, solutes are getting retarded very strongly nearer to the inlet itself, and the solutes are not allowed to migrate too far from the inlet. It is observed from Fig. 4 that first few days seem to be very critical in deciding the resultant effective solute velocity depending on the intensity of sorption partition coefficients, while the magnitude of effective solute velocity is not getting affected significantly at a later stage.

Fig. 5 provides the temporal distribution of effective macro-dispersion coefficient within the high permeable fracture for various sorption partition coefficients. The macro-dispersion coefficients for the ranges of sorption partition coefficients considered in Fig. 5 vary quite significantly nearer to the inlet, while their values try to reach a steady-state at a later time. It is observed from Fig. 5 that the intensity of mixing for all the sorption partition coefficients is less than the normal mixing that will be expected in the absence of any physical/chemical reactions. In other words, the sorption partition coefficients suppress the dilution of solute concentrations. As observed from Fig. 5, for a larger sorption partition coefficient (K_s = 2), the effective macro-dispersion coefficient has mitigated by more than an order of magnitude. Thus numerical results clearly suggest that the role of sorption partition coefficients is not always enhancing the mixing phenomena which lead to dilution of solutes.

Fig. 6 provides the temporal distribution of effective dispersivity within the high permeable fracture for various sorption partition coefficients. The effective dispersivity for the ranges of sorption partition coefficients considered in Fig. 6 varies non-linearly with time throughout the simulation period. It is observed from Fig. 6 that the magnitude of effective dispersivity keeps on increasing significantly with time for very low sorption partition coefficient, while the magnitude of effective dispersivity is less than its actual value for significantly higher sorption partition coefficients. Thus these numerical results suggest that the role of sorption partition coefficients is extremely sensitive in the sense that the resultant magnitude of effective dispersivity may either get enhanced or mitigated depending on the magnitude of sorption partition coefficients. Such results are relatively difficult to deduce from field investigations as it needs more number of experimental investigations and eventually, the critical role of numerical models is justified.

Fig. 7 provides spatial distribution of relative concentration along the fracture resulting from the introduction of non-linear Langmuir sorption isotherm within fracture, fracture–skin and rock-matrix for various maximum sorption capacities. It can be clearly observed from Fig. 7 that the magnitude of maximum sorption capacities plays a major role in deciding the amount of concentration that would finally be retained within the fracture. For example, the relative concentration at a distance of 2.5 m from the inlet nearly approaches zero with S_{maxs} = 0.01; while the relative concentration is approximately 60% with S_{maxs} = 0.00001. Thus the role of non-linear sorp-

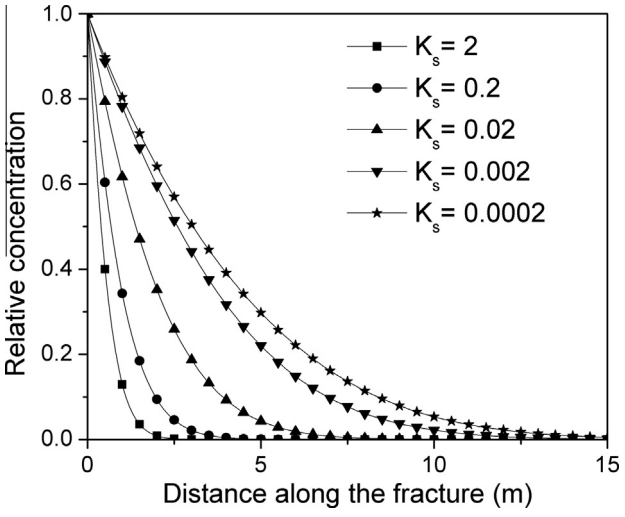

Figure 3 Spatial distribution of relative concentration along the fracture for various sorption partition coefficients within the fracture skin.

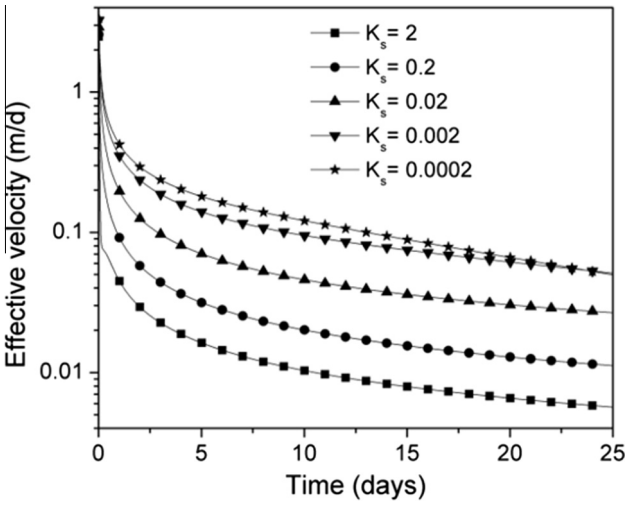

Figure 4 Temporal distribution of effective solute velocity for different sorption partition coefficients in the fracture skin.

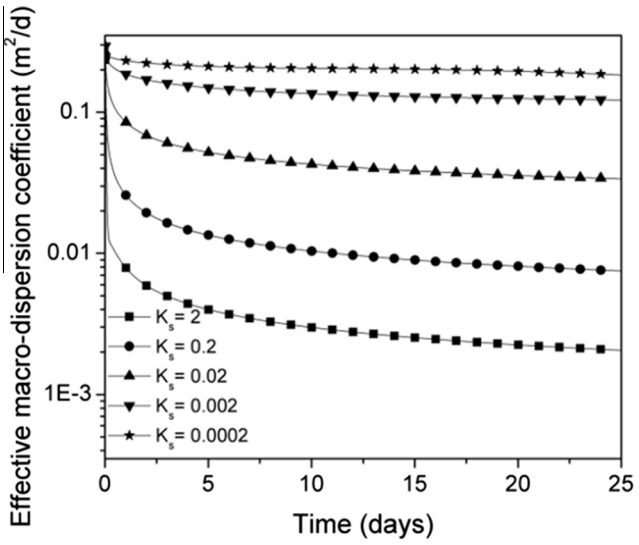

Figure 5 Temporal distribution of effective solute macro-dispersion coefficients for different sorption partition coefficients in the fracture skin.

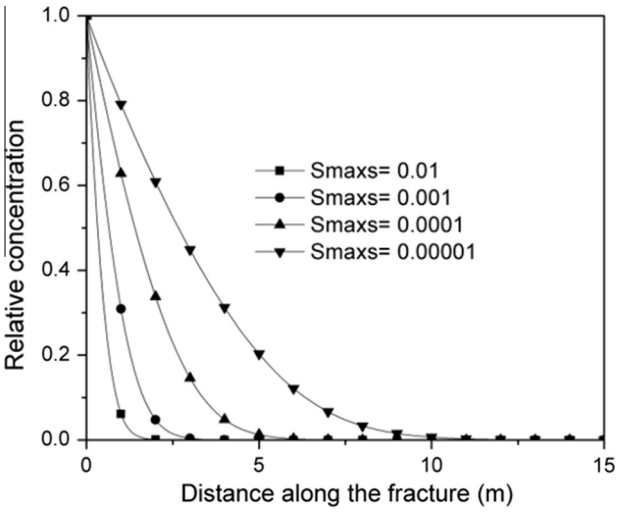

Figure 7 Spatial distribution of relative concentration along the fracture for various maximum sorption capacities within the fracture skin.

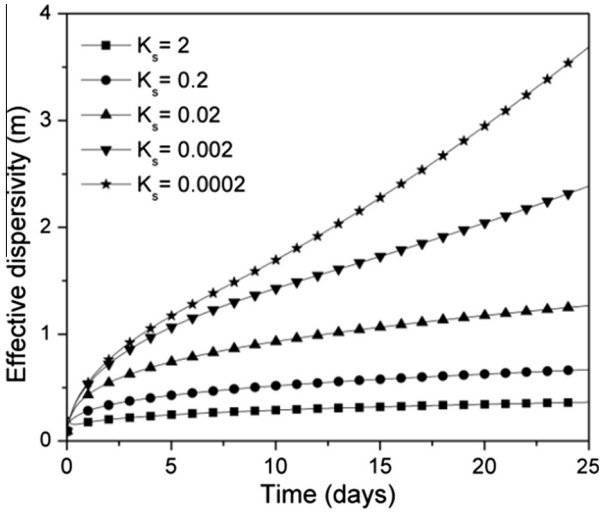

Figure 6 Temporal distribution of effective solute dispersivity for different sorption partition coefficients in the fracture skin.

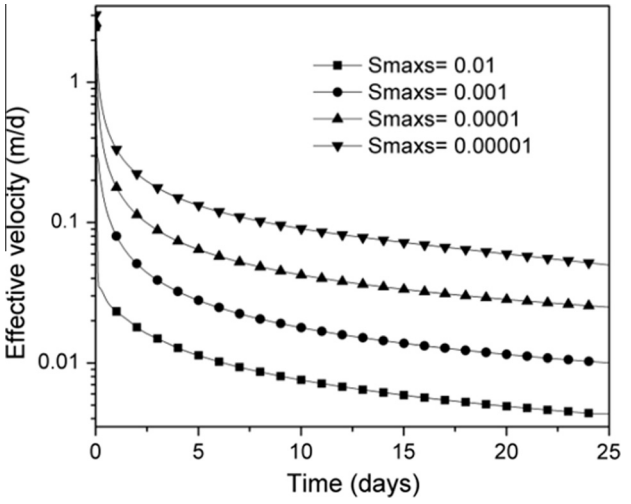

Figure 8 Temporal distribution of effective solute velocity for different maximum sorption capacities in the fracture skin.

tion is dominant in comparison with that of advection and dispersion in deciding the final relative concentration within the fracture. In addition, it is also observed that the concentration reaches zero within 10 m from the inlet for all the maximum sorption capacities considered in Fig. 7 implying a very strong sorption onto the solid phase from the mobile aqueous phase.

Fig. 8 provides the temporal distribution of effective solute velocity within the high permeable fracture for various maximum sorption capacities. The effective solute velocity for the ranges of sorption partition coefficients considered in Fig. 8 varies non-linearly implying the sensitivity of effective solute velocity with time. It is observed from Fig. 8 that the magnitude of effective solute velocities is nearly two orders of magnitude lower with reference to its mean fluid velocity of 1 m/day. In addition, solutes are getting retarded very strongly during first 5–10 days, and the solutes move at a very slow rate at times greater than 10 days. It is observed from Fig. 8 that the first week is very critical in deciding the resultant effective solute velocity depending on the intensity of maximum sorption capacities, while the magnitude of effective solute velocity is not getting affected significantly at a later stage.

Fig. 9 provides the temporal distribution of effective macro-dispersion coefficient within the high permeable fracture for various maximum sorption capacities. The macro-dispersion coefficients for the ranges of maximum sorption capacities considered in Fig. 9 vary quite significantly nearer to the inlet, while their values try to reach a steady-state at a later time. It is observed from Fig. 9 that the intensity of mixing for all the maximum sorption capacities is less than the normal mixing that will be expected in the absence of any physical/chemical reactions. In other words, the maximum sorption capacities suppress the dilution of solute concentrations as observed in Fig. 5. As observed from Fig. 9, for a lar-

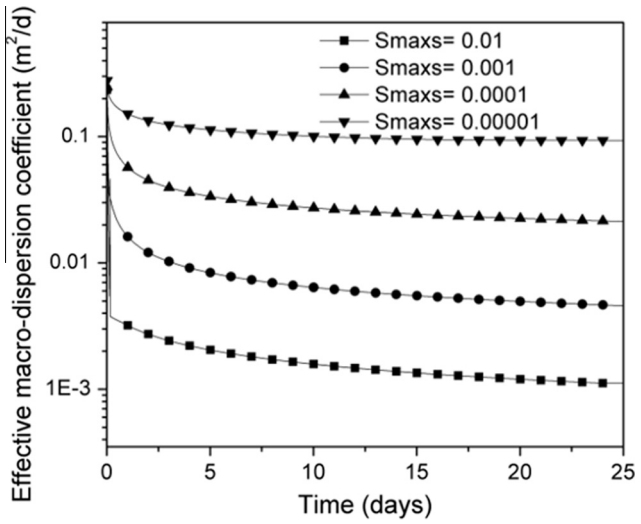

Figure 9 Temporal distribution of effective macro-dispersion coefficient for different maximum sorption capacities in the fracture skin.

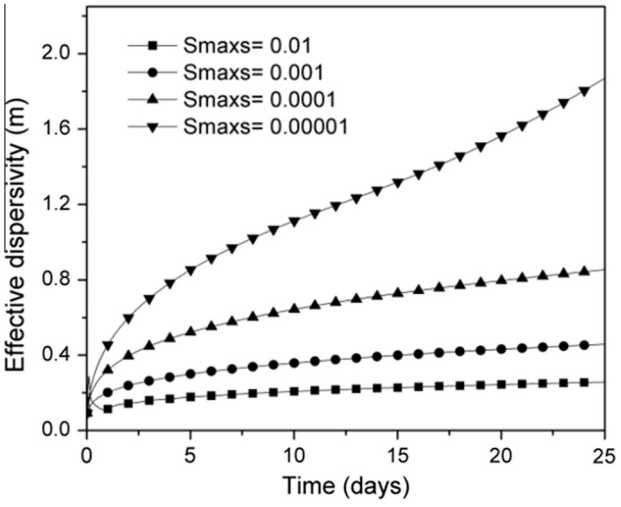

Figure 10 Temporal distribution of effective solute dispersivity for different maximum sorption capacities in the fracture skin.

ger maximum sorption capacity (S_{maxs} = 0.01), the effective macro-dispersion coefficient has mitigated by nearly two orders of magnitude. Thus numerical results clearly suggest that the role of maximum sorption capacities is not always enhancing the mixing phenomena which lead to dilution of solutes.

Fig. 10 provides the temporal distribution of effective dispersivity within the high permeable fracture for various maximum sorption capacities. The effective dispersivity for the ranges of sorption partition coefficients considered in Fig. 10 varies non-linearly with time throughout the simulation period. It is observed from Fig. 10 that the magnitude of effective dispersivity keeps on increasing significantly with time for very low maximum sorption capacity (S_{maxs} = 0.00001), while the magnitude of effective dispersivity is less than its actual value for significantly higher maximum sorption capacities (S_{maxs} = 0.001 and 0.01). Thus these numerical results suggest that the role of maximum sorption capacities is extremely sensitive in the sense that the resultant magnitude of effective dispersivity may either get enhanced or mitigated depending on the magnitude of maximum sorption capacities. Thus the maximum sorption capacities play a critical role with reference to any conclusion pertaining to scale-dependent dispersivity.

5. Conclusion

A numerical model is developed to analyse the effect of Langmuir non-linear sorption intensities on the effective solute velocity, macro dispersion coefficient and dispersivity in a fracture–skin–matrix coupled system. The set of coupled equations for contaminant transport is solved using the implicit finite difference method. A constant continuous source of contaminants is assumed at the inlet of the fracture. The flux transfer at the interface of the fracture and the fracture–skin is captured by adopting a varying grid pattern. The fractures are assumed to be saturated. The conclusions from the study can be summarized as follows:

1. The role of non-linear sorption is dominant in comparison with that of advection and dispersion in deciding the final relative concentration within the fracture.
2. Higher sorption partition coefficients try to suppress the enhanced mixing phenemona, and subsequently, the amount of mixing pertains to actual hydrodynamic dispersion coefficient as observed in the absence of any physical/chemical reactions.
3. The first few days seem to be very critical in deciding the resultant effective solute velocity depending on the intensity of sorption partition coefficients, while the magnitude of effective solute velocity is not getting affected significantly at a later stage.
4. The role of sorption partition coefficients is not always enhancing the mixing phenomena which lead to dilution of solutes.
5. The role of sorption partition coefficients is extremely sensitive in the sense that the resultant magnitude of effective dispersivity may either get enhanced or mitigated depending on the magnitude of sorption partition coefficients.

References

Abulaban, A., Nieber, J.L., 2000. Modeling the effects of nonlinear equilibrium sorption on the transport of solute plumes in saturated heterogeneous porous media. Adv. Water Resour. 23, 893–905.

Abulaban, A., Nieber, J.L., Misra, D., 1998. Modeling plume behaviour for nonlinearly sorbing solutes in saturated homogeneous porous media. Adv. Water Resour. 21, 487–498.

Brusseau, M., 1995. The effect of nonlinear sorption on transformation of contaminants during transport in porous media. J. Contam. Hydrol. 17, 277–291.

Guven, O., Molz, F.J., Melville, J.G., 1984. An analysis of dispersion in a stratified aquifer. Water Resour. Res. 20, 1337–1354.

Maloszewski, P., Zuber, A., 1985. On the theory of tracer experiments in fissured rocks with a porous matrix. J. Hydrol. 79, 333–358.

Patnaik, L.N., Das, C.P., 1995. Removal of hexavalent chromium by Blast Furnace flue dust. Indian J. Environ. Health 37, 19–25.

Renu, V., Suresh Kumar, G., 2012. Numerical modelling and spatial moment analysis of solute mobility and spreading in a coupled fracture–skin–matrix system. Geotech. Geol. Eng. 30, 1289–1302.

Robinson, N.I., Sharp Jr., J.M., 1997. Analytical Solution for Contaminant Transport in a Finite Set of Parallel Fractures with Matrix Diffusion, C.S.I.R.O. Mathematical and Information Sciences, Report CMIS-C23, pp. 26.

Satter, A., Shum, Y.M., Adams, W.T., Davis, L.A., 1980. Chemical transport in porous media with dispersion and rate-controlled adsorption. SPE 20, 129–138.

Sekhar, M., Suresh Kumar, G., Misra, D., 2006. Numerical modelling and analysis of solute velocity and macro-dispersion for linearly and non-linearly sorbing solutes in a single fracture with matrix diffusion. J. Hydrol. Eng. 11, 319–328.

Sekhar, M., Suresh Kumar, G., 2006. Modeling transport of linearly sorbing solutes in a single fracture: asymptotic behavior of solute velocity and dispersivity. Geotech. Geol. Eng. 24, 183–201.

Singh, D.K., Srivastava, B., 2001. Basic dyes removal from wastewater by adsorption on rice husk carbon. Indian J. Chem. Technol. 8, 133–139.

Srivastava, R., Brusseau, M.L., 1996. Nonideal transport of reactive solutes in heterogeneous porous media: 1. Numerical model development and moments analysis. J. Contam. Hydrol. 24, 117–143.

Srivastava, R., Sharma, P.K., Brusseau, M.L., 2002. Spatial moments for reactive transport in heterogeneous porous media. J. Hydrol. Eng. 7, 336–341.

Suresh Kumar, G., 2008. Effect of sorption intensities on dispersivity and macro-dispersion coefficient in a single fracture with matrix diffusion. Hydrogeol. J. 16, 235–249.

Suresh Kumar, G., Sekhar, M., Misra, D., 2008. Time dependent dispersivity of linearly sorbing solutes in a single fracture with matrix diffusion. J. Hydrol. Eng. 13, 250–257.

Suresh Kumar, G., Sekhar, M., 2005. Spatial moment analysis for transport of nonreactive solutes in a fracture–matrix system. J. Hydrol. Eng. 10, 192–199.

Weber, W.J.J., McGinley, P.M., Katz, L.E., 1991. Sorption phenomena in subsurface systems: concepts, models and effects on contaminant fate and transport. Water Res. 25, 499–528.

Moench, A.F., 1984. Double-porosity models for a fissured groundwater reservoir with fracture skin. Water Resour. Res. 20, 831–846.

Moench, A.F., 1985. Convergent radial dispersion in a double-porosity aquifer with fracture skin: analytical solution and application to a field experiment in fractured chalk. Water Resour. Res. 31, 1823–1835.

Robinson, N.I., Sharp Jr, J.M., Kriesel, I., 1998. Contaminant transport in a set of parallel fractures with fracture skin. J. Contam. Hydrol. 31, 83–109.

Sharp, J.M., 1993. Fractured aquifers/reservoirs: approaches, problems, and opportunities. In: Banks, D., Banks, S. (eds) Hydrogeology of Hard Rocks, Memoires of the 24th Cong. International Assoc. Hydrogeologists. Oslo, Norway 24, pp. 23–38.

Fu, L., Milliken, K.L., Sharp Jr, J.M., 1994. Porosity and permeability variations in the fractured and liesegang-banded Breathitt Sandstone (Middle Pennsylvanian), eastern Kentucky: diagenetic controls and implications for modelling dual porosity systems. J. Hydrol. 154, 351–381.

Driese, S.G., McKay, L.D., Penfield, C.P., 2001. Lithologic and pedogenic influences on porosity distribution and groundwater flow in fractured sedimentary saprolite: a new application of environmental sedimentology. J. Sediment Res. 71, 843–857.